

The Wide-Field Imager for IXO: Status and future activities

Lothar Strüder^{*ab}, Florian Aschauer^{ab}, Mark Bautz^c, Luca Bombelli^d, David Burrows^e, Carlo Fiorini^d, George Fraser^f, Sven Herrmann^{ab}, Eckhard Kendziorra^h, Markus Kusterⁱ, Thomas Lauf^{ab}, Peter Lechner^j, Gerhard Lutz^j, Petra Majewski^j, Aline Meuris^{ab}, Matteo Porro^{ab}, Jonas Reiffers^{ab}, Rainer Richter^{bk}, Andrea Santangelo^h, Heike Soltau^j, Alexander Stefanescu^{bl}, Chris Tenzer^h, Johannes Treis^{bm}, Hiroshi Tsunemiⁿ, Giulio de Vita^{ab}, Jörn Wilms^o

^a Max-Planck-Institut für extraterrestrische Physik, Giessenbachstr., 85741 Garching, Germany;

^b MPI Halbleiterlabor, Otto-Hahn-Ring 6, 81739 München, Germany;

^c Kavli Institute for Astrophysics and Space Research, Massachusetts Institute of Technology, Cambridge, MA 02139, USA;

^d Politecnico di Milano, Dipartimento di Elettronica e Informazione, Via Golgi 40, 20133 Milan, Italy;

^e Pennsylvania State University, Astronomy Department, University Park, Pennsylvania 16802, USA;

^f University of Leicester, University Road, LE1 7RH Leicester, UK;

^h Institut für Astronomie und Astrophysik, Universität Tübingen, D-72076 Tübingen, Germany;

ⁱ XFEL GmbH, Notkestrasse 85, 22607 Hamburg, Germany;

^j PNSensor GmbH, Römerstr. 28, 80803 München, Germany;

^k Max-Planck-Institut für Physik, Föhringer Ring 6, 80805 München, Germany;

^l J.-Gutenberg-Universität, Institut für anorganische und analytische Chemie, 55099 Mainz, Germany;

^m Max-Planck-Institut für Sonnensystemforschung, Max-Planck-Str.2, 37191 Katlenburg-Lindau, Germany;

ⁿ Department of Earth and Space Science, Graduate School of Science, Osaka University, Toyonaka, Osaka 560-0043, Japan;

^o Erlangen Centre for Astroparticle Physics, Erwin-Rommel-Str. 1, 91058 Erlangen, Germany.

ABSTRACT

The Wide Field Imager (WFI) of the International X-ray Observatory (IXO) is an X-ray imaging spectrometer based on a large monolithic DePFET (Depleted P-channel Field Effect Transistor) Active Pixel Sensor. Filling an area of 10 x 10 cm² with a format of 1024 x 1024 pixels it will cover a field of view of 18 arcmin. The pixel size of 100 x 100 μm^2 corresponds to a fivefold oversampling of the telescope's expected 5 arcsec point spread function. The WFI's basic DePFET structure combines the functionalities of sensor and integrated amplifier with nearly Fano-limited energy resolution and high efficiency from 100 eV to 15 keV. The development of dedicated control and amplifier ASICs allows for high frame rates up to 1 kHz and flexible readout modes. Results obtained with representative prototypes with a format of 256 x 256 pixels are presented.

Keywords: International X-ray Observatory, IXO, Wide Field Imager, WFI, X-ray Astronomy, X-ray Spectroscopy, X-ray Imaging, DePFET, Active Pixel Sensor

1. INTRODUCTION

The International X-ray Observatory (IXO) ^[1] is a joint effort by NASA, ESA and JAXA to build a next-generation observatory-class X-ray mission. IXO will investigate high-energy phenomena in the X-ray band characterizing the evolution of cosmic structures on both large and small scales with unprecedented detail and precision. Three primary science goals have been defined for IXO: black holes and matter under extreme conditions, the formation and evolution of galaxies, clusters and large scale structure, and the life cycles of matter and energy.

* corresponding author, lts@hll.mpg.de; phone +49.89.83940041; www.hll.mpg.de.

IXO is supposed to be launched in 2021 to a halo orbit around the second Lagrange point (L2) of the sun-earth system. The mission's key component is a Wolter-type-I X-ray mirror system with an effective area of 3 m^2 at 1.25 keV, a focal length of 20 m, and high angular resolution with a point spread function (PSF) of 5 arcsec half energy width. To cover the multitude of scientific tasks IXO's baseline instrumentation foresees a suite of six specialized instruments:

- The Wide Field Imager (WFI) is a Silicon Active Pixel Sensor (APS) detector covering a very large field of view of 18 arcmin with excellent spectral resolution (130 eV FWHM at 5.9 keV), and good imaging resolution (5-fold oversampling of the mirror point spread function) in the energy range from 100 eV to 15 keV.
- The Hard X-ray Imager (HXI) is based on a double-sided CdTe strip detector in combination with Si strip and BGO anticoincidence detectors. It offers an 8 arcmin field of view with an energy resolution $< 1 \text{ keV}$ FWHM at 30 keV. The HXI is mounted behind the WFI and will extend IXO's energy coverage to the energy band of 15 – 40 keV.
- The X-ray Microcalorimeter Spectrometer (XMS) is a non-dispersive high-resolution imaging spectrometer using an array of superconductive Transition Edge Sensors (TES). It has a spectral resolution in the eV-range and covers a field of view of 5 arcmin.
- The High Time Resolution Spectrometer (HTRS) is a monolithic array of 31 Silicon Drift Detectors (SDDs) foreseen for timing and spectroscopy studies of bright point sources. It is a non-imaging spectrometer with a large sensitive area of 4.5 cm^2 , good energy resolution (150 eV FWHM at 5.9 keV), timing resolution of 10 μsec and high count rate capability up to 10^6 per second without pileup limitation. The sensor is placed on axis but out of focus so that the converging beam from the mirror is distributed uniformly across the SDD array.
- The X-ray Polarimeter (XPol) is an imaging polarimeter based on a fine grid gas pixel detector with a field of view of 2.6 arcsec. The XPol measures the polarization of the incident X-ray photons on a sensitivity level of 1 % by imaging the photo-electron tracks.
- The X-ray Grating Spectrometer (XGS) is a non-imaging dispersive high resolution spectrograph. It diffracts light out of the main optical path onto its CCD detector array. The effective XGS area is 1000 cm^2 (0.3 – 1.0 keV). It offers a very high spectral resolution of $\lambda/\Delta\lambda = 3000$.

Five of the instruments (XMS, the combined WFI/HXI, HTRS, and XPol) are placed on a Moveable Instrument Platform (MIP) rotating the selected instrument into the focus. Science data will be collected using one of the MIP-mounted instruments at a time. The XGS-CCD camera is placed on the Fixed Instrument Platform and will operate simultaneously with the observing MIP instrument.

2. THE IXO WIDE FIELD IMAGER

The IXO wide field imager is an imaging X-ray spectrometer with a large field of view. The purpose of the WFI is to provide images over a broad energy band from 100 eV to 15 keV, simultaneously with spectrally and time resolved photon counting. Being an on-axis imaging instrument, the WFI is mounted on the Moveable Instrument Platform (MIP) and is moved into the optical path on demand. IXO's large collecting area and high angular resolution set demanding instrument requirements:

- To detect X-ray luminous objects at high red-shift, which are expected to have a density of one per 5 arcmin section of the sky, and to provide sufficient background statistics the WFI sensor must cover a large field of view. The IXO specification is a 18 arcmin field of view translating to a sensitive area of more than 10 cm diameter in the focal plane.
- To limit source confusion and to resolve red-shifted objects the telescope's angular resolution must be a half energy width (HEW) of 5 arcsec, corresponding to a $500 \mu\text{m}$ wide point spread function in the focal plane. A pixel size of $100 \mu\text{m}$, i.e. an oversampling of the point spread function by a factor of five, is adequate to ensure that the spatial resolution is limited by the telescope rather than by the sensor.
- The WFI must provide efficient response in the energy range from 100 eV to 15 keV requiring a thin radiation entrance window and a sensitive thickness of $450 \mu\text{m}$.

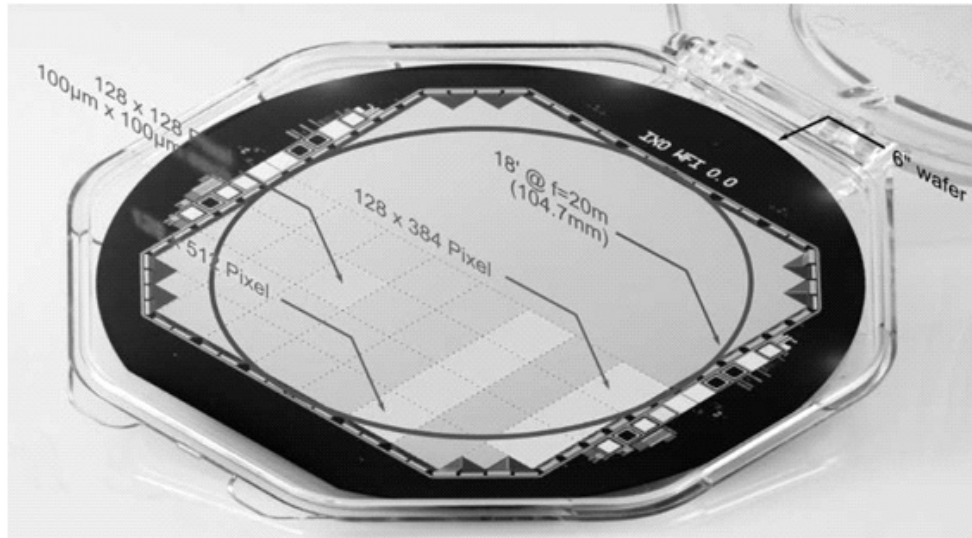


Figure 1. Mechanical sample of the IXO WFI 6-inch wafer-scale detector. Plotted over one hemisphere is the logical layout of the detector. It consists of roughly 1024 x 1024 pixels of 100 x 100 μm^2 size. The sensor is logically subdivided into two hemispheres, consisting of 8 sectors each. Every sector is read out by a dedicated readout ASIC. To facilitate the monolithic integration, the corners of the detector must be left free. Shown here are two options: The plotted graphics shows corners with 128x128 pixels per corner left free, the photograph shows a more complicated option based on 64 x 64 pixels subunits.

- Spectroscopy of relativistic distorted lines requires an electronic noise < 10 electrons ENC (equivalent noise charge) corresponding to spectral line width of 150 eV FWHM at 5.9 keV.
- To avoid photon pileup the full frame readout time must be in the order of msec. For instance, at a frame rate of 1000 Hz a source producing 1000 counts per sec on an area of 7 x 7 pixels can be detected with a pile-up probability below 2 % in full frame mode. To cope with high-intensity point sources a fast window mode, comprising a depth of e.g. 16 pixels, must be implemented.
- The presence of the HXI instrument detecting the high-energy photons transmitted through the WFI sensor implies that the WFI sensor must be a monolithic device without mechanical support structure below the sensitive area.

To unify these specifications in a single device the baseline WFI concept foresees a Silicon Active Pixel Sensor (APS), i.e. every pixel has its own integrated amplifier and can be addressed individually. The WFI sensor will have a format of 1024 x 1024 pixels with a pixel size of 100 μm x 100 μm equal to a sensitive area of 10.24 cm x 10.24 cm (fig. 1). It will be a monolithic device processed on a 6-inch silicon wafer with a thickness of 450 μm . To facilitate the monolithic integration, each corner of the detector has an area of the size of 128 x 128 pixels that is left free. As this area lies outside of the nominal FoV of the X-ray optics, it is shaded by the baffle system of the X-ray telescope, and the free corners do not limit the usable FoV.

The sensor area is logically divided into two hemispheres with 512 rows and 1024 columns, each consisting of eight subunits with a format of 128 x 512 pixels (128 x 384 pixels for the four corner subunits, fig. 1). Every subunit is readout by a dedicated read out ASIC. To provide a high frame rate, both hemispheres are read out in parallel. As the detector is backside illuminated and the hemispheres and subunits are only extrinsic structures on a homogeneous pixel array, the geometrical fill factor and the quantum efficiency are not affected by this division.

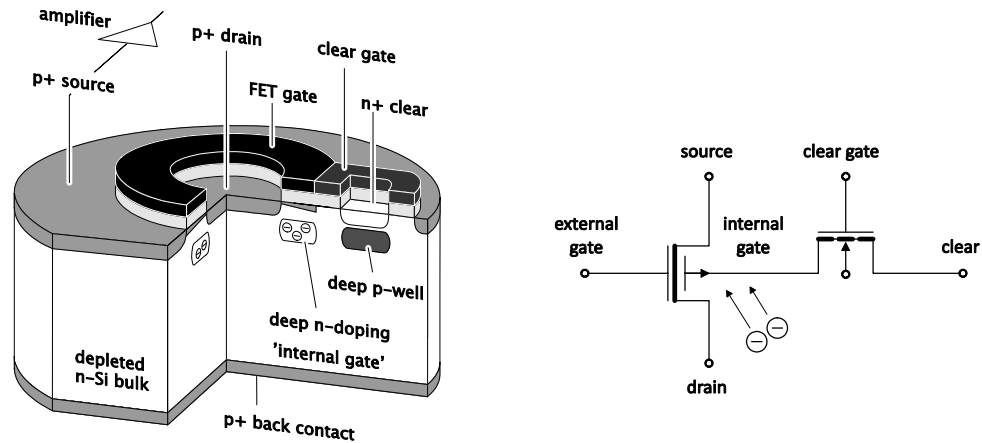


Figure 2. Principle view of a DEPFET and its equivalent circuit.

3. THE DEPFET PRINCIPLE

The DePFET (DEpleted P-channel Field Effect Transistor) is a device with the combined functionality of detector and amplifier^[2]. It consists of a p-channel field effect transistor on a high resistivity n-type silicon bulk. The transistor may be either a JFET or a MOSFET of enhancement or depletion type. For reasons of technological feasibility and reproducibility on large scale devices the MOSFET-based device is usually the preferred design. The bulk is completely depleted by the reverse biased backside diode. That way a potential minimum for electrons is created close to the surface. An additional deep n-doped region enhances the depth of the potential minimum and confines it in the lateral direction to the extent of the FET channel (fig. 2).

Each electron generated in the depleted volume, either thermally or by the absorption of ionizing radiation, will drift to the potential minimum and will be stored there. By inducing positive image charges inside the FET channel the stored electrons enhance the transistor current. Thus the DePFET's current is a function of the amount of charges in the potential minimum, and its measurement yields information of the energy absorbed in the depleted volume. Because of the stored electrons' current steering function the potential minimum is called 'internal gate'. As the signal charges are confined in an isolated potential well, the information is available for readout on demand.

To reset the DePFET electrons accumulated in the internal gate must be periodically removed by applying a suitable high voltage to an n⁺-doped 'clear' contact adjacent to the internal gate. The clear contact acts as a drain for electrons and it is supported by an additional MOS 'clear gate'. For the reset, both the clear contact and the clear gate are pulsed to a more positive voltage. To inhibit the direct loss of signal electrons and the back injection of electrons to the internal gate the clear contact is shielded by a deep p-implanted well.

The internal gate exists, i.e. electrons can be collected and stored in it, regardless of a current flowing in the channel of the DePFET or not. The transistor current is usually turned off during signal integration and only switched on via the external gate for the signal readout, thus minimizing the power consumption. Unlike a conventional detector-preamplifier system the DePFET is free of interconnection stray capacitances and the overall capacitance is minimized.

4. DEPFET-BASED ACTIVE PIXEL SENSOR

In the context of the IXO Wide Field Imager the DePFET structure is used as the unit cell of an Active Pixel Sensor (APS) with random accessible pixels, flexible readout mode, and high energy and spatial resolution, suitable to cope with the challenging requirements. All pixels have a common bulk and back contact. As the bulk is fully depleted the sensor is irradiated through the homogeneous, non-structured, thin backside entrance window. The two-dimensional pixel array has no insensitive gaps, and the DePFET APS has a fill factor of 100 %.

Since the signal charge is both stored and read out in the DePFET, each pixel of a two-dimensional matrix of pixels can in principle be read out individually. However, as pixel-individual connections would require a very high amount of routing resources and pixel-individual readout is not required in the scenario of the WFI, a simple interconnected matrix readout scheme is foreseen for the WFI. Therefore, the matrix of DePFETs is organised for column-parallel readout, i.e., all the pixels in one row are processed simultaneously, by row-wise connection of the external DePFET gates, the clear contacts and the clear gates. The readout nodes (either drain or source, both options are available and investigated) are connected column-wise (fig. 3). In normal operation one row of pixels is selected for readout and reset while the rest of the pixels is turned off but still integrating signal charges. The integration time of a pixel is equal to the number of pixel rows multiplied by the time required for readout and reset of one row.

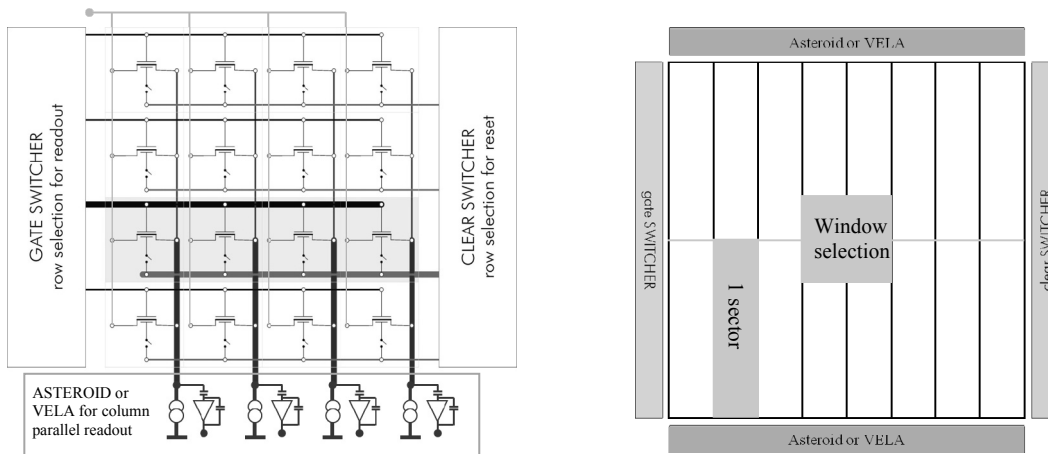


Figure 3. (Left) Principle of readout of a DePFET matrix. Gates, clear contacts and clear gates are connected row-wise to control units, readout nodes (source or drain) are connected column-wise to a readout chip. One row is selected for readout and reset, while the remaining pixels are integrating signals. Pixels can be addressed individually. (Right) Implementation for the wide-field imager. The matrix is logically divided in 16 sectors, each one read out by one analog front-end Asic. Window modes can be implemented on the matrix to read at a higher rate a small part of the device.

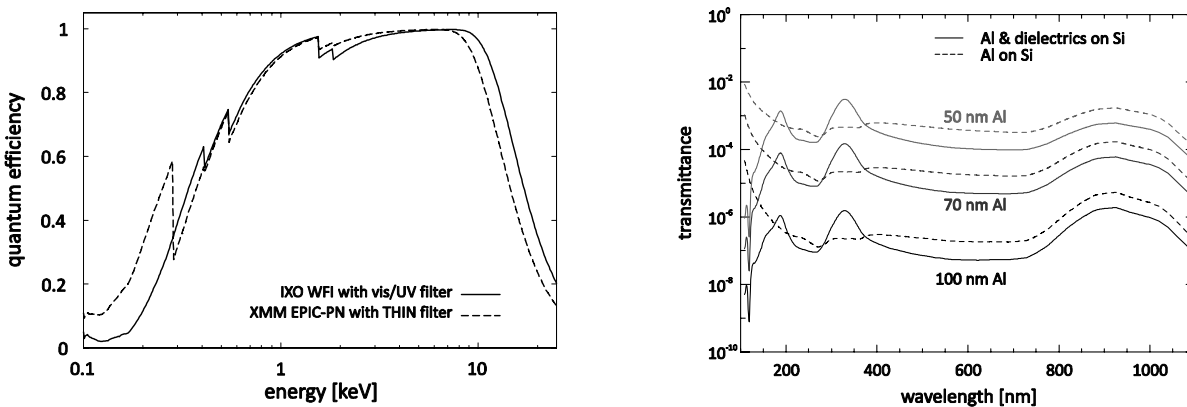


Figure 4. Expected WFI quantum efficiency curve (left) with an assumed UV/optical blocking filter (70 nm Al + SiO₂/Si₃N₄ multilayer coating). Shown for comparison is the XMM quantum efficiency, using the thin optical blocking filter. The difference at the high energy side is due to the increased bulk thickness of the WFI detector (450 μ m to be compared to 280 μ m). The figure to the right shows the optical transmittance for various filter configurations.

The device is fully depleted using the sideways depletion principle, allowing signal charges generated by radiation entering from the backside of the detector to be detected efficiently. Backside illuminating the detector in this way allows the APS to have a geometrical fill factor of 100 %. Furthermore, this allows for using a very thin entrance window with consequently very good quantum efficiency over a wide energy range (fig. 4). The large thickness of the fully depleted bulk provides for high quantum efficiency in the regime above 10 keV. A beneficial side-effect of backside-illumination is self-shielding. As the radiation absorbed in the bulk does not reach the structures on the front-side, radiation hardness is intrinsically improved. As the large effective area X-ray mirror system does not only focus X-rays but also visible and UV light, care must be taken to avoid problematically high optical photon loads. Therefore, an optical blocking filter system consisting of a thin Al-layer on top of an UV blocking system consisting of a Silicon Oxide/Nitride multi-layer coating is foreseen (fig. 4).

Compared to CCDs the DePFET APS has the intrinsic advantage of signal charge amplification at the position of its generation thus avoiding any charge transfer over macroscopic distance where losses and out-of-time events could occur. In addition the APS pixels are individually addressable, and the application of any kind of windowing or sparse readout is possible, while in a CCD the access to the individual pixel contents is strictly sequential.

5. THE DEPFET APS READOUT AND CONTROL SYSTEM

5.1 Readout electronics

The signal information stored in the internal gate is extracted by a measurement of the DePFET current. A baseline subtraction is obtained by a consecutive read-clear-read sequence: First, the current level given by a baseline value plus the additional current induced by the signal charges in the internal gate is read out. Next, the clear operation is performed by applying positive pulses to the clear contacts and the clear gates. Finally, the baseline current at empty internal gate is measured. The charge information is obtained from the current difference before and after the clear process. As the baseline is read after the signal the clear process affects the noise performance of the device significantly. To avoid kTC reset noise the entire signal charge must be removed from the internal gate completely, otherwise an additional noise contribution occurs due to an undefined amount of remaining charge in the internal gate. The required full clear has been demonstrated with existing DePFET prototypes^[3]. To sense the DePFET current two basic circuits are available and have been translated into hardware in two 64-channel analog frontend chips implementing one preamplifier, one filter amplifier and a sample & hold circuit per channel followed by a sequencer controlled analog 64/1 multiplexer. One of the designs, the VLSI Electronics for Astronomy (VELA)^[4] is designed for drain current readout and directly integrates the current provided by the pixel device. To use the amplifier's dynamic range more efficiently, the offset current of the pixel is subtracted prior to signal acquisition. The other design, called ASTEROID (Active current Switching TEchnique ReadOut In X-ray spectroscopy with DePFET)^[5], implements the source follower readout scheme using the same shaper, but a combination of a first stage amplifier and a voltage-to-current converter for interfacing source follower and shaper. In spite of their different input stages, both ICs have identical filtering stages. The readout time per pixel row obtained with current versions of the frontend chips are 2 μ sec for the VELA and 4 μ sec for the ASTEROID. Both versions will be further developed in parallel. A decision will be made in a later stage of the project. Both circuits The WFI baseline foresees the final readout chip to be manufactured in a 128-channel version with two analog outputs to be connected to external ADCs. For the split-frame readout of the WFI hemispheres a total of 16 frontend ASICs will be applied.

5.2 Control electronics

DePFET pixels are controlled by toggling a sequence of voltages on the gate, clear gate and clear contacts of each row. The correct sequence of voltages is applied by the SWITCHER ASIC, a 64-channel, dual output, high voltage switching circuit in rad-hard design and manufactured in an AMS 0.3 μ m/3.3 V CMOS process using a high-voltage option. The SWITCHER is a DePFET-specific development and able to toggle the output between two individual voltages each with a difference of 20 V at a maximum frequency of 20 MHz. The programming of the SWITCHER is flexible in the choice of arbitrary row patterns so that any kind of windowing can be applied. For the operation of large format APSs a number of SWITCHER chips can be daisy-chained and performs as one large device. The WFI baseline foresees the SWITCHER control chip to be manufactured in a 128-channel version with a number of 16 ASICs supplying the clocked gate, clear and clear-gate voltages.

5.3 Data Acquisition

When the FPA is operated, each of the 32 AFE ASIC outputs generates a stream of 64 analog voltages per row. At the targeted integration time of $2.5 \mu\text{s}$ per row and assuming an upper limit of 16 bit digitization, this corresponds to a raw data rate of more than 1.5 Gbyte/s. It is immediately obvious that the raw data must be efficiently reduced at an early stage.

In the first step of data processing, a set of FPGAs perform simple, serial-data oriented DAQ tasks like noise, threshold and offset calculations and offset and gain corrections. The first stage FPGAs join the data streams from four ADCs each, and, together with their ADCs, form a total of eight ADC Clusters.

In a second step, the data streams from the four ADC clusters of each hemisphere are aggregated by a Framelet Builder FPGA. In this FPGA, data reduction steps requiring knowledge about neighboring pixels are performed. Pixels exceeding a threshold value are identified and flagged as seed pixels. The neighborhood around all seed pixels is transferred to a third stage data reduction, while all pixels not near a seed pixel are discarded. As each Framelet Builder has no knowledge of the other's hemisphere, additionally all pixels near the hemisphere border are transmitted.

In the third stage data processing, a Frame Builder FPGA joins the data from the two Framelet Builders. Seed patterns spanning the hemisphere border are detected, and the final zero suppression is performed. After this, more complex data analysis routines operate on the remaining events. Hit patterns are recognized and classified, further corrections for sensor or FEE specific properties can be implemented, and the final frames are assembled, time-stamped, and compressed in preparation for telemetry.

The entire WFI is controlled by the Brain module, containing the main instrument control, the housekeeping, the communication with the spacecraft environment, control of the power supplies and the main sequencer for the data acquisition. It controls and configures also the sequence of acquisition modes, the setting of ROI windows and the repetition rate of their readout.

6. PROTOTYPE DEVICE STATUS

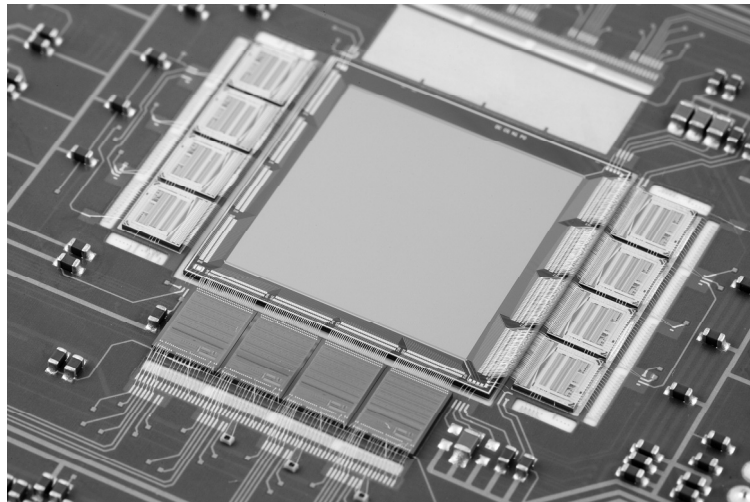


Figure 5. Photograph of an APS hybrid with the 256×256 sensor chip in the center, eight SWITCHER control chips for readout/reset selection of one pixel row (left and right), and four 64-channel ASTEROID readout chips at the bottom. The pixel size is $75 \times 75 \mu\text{m}^2$, the sensitive area is $1.92 \times 1.92 \text{ cm}^2$.

Since the beginnings of DePFET development, a large variety of devices, from single pixels and small APS prototypes with a format of 64×64 pixels and a pixel size of $75 \mu\text{m}$ devices^[3] up to large DePFET Macropixel arrays consisting of 64×64 pixels with $500 \mu\text{m}$ pixel size and having an overall sensitive area of $3.2 \times 3.2 \text{ cm}^2$ ^[6], have been built and tested at the MPI semiconductor lab. The production yield was generally very good. Cosmetic defects, e.g. bright or noisy

pixels, were very rare, making most devices perfect. The devices show near Fano-limited energy resolution even at fast readout speeds.

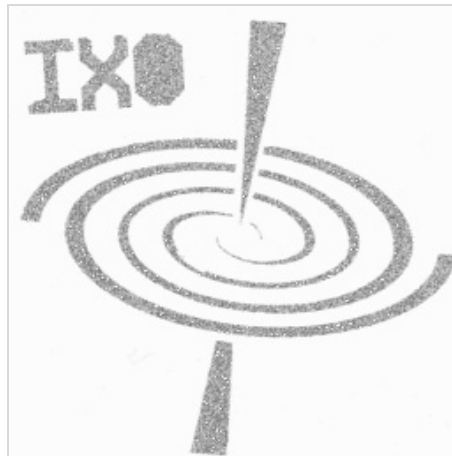


Figure 6. Shadow image acquired with the device shown in fig. 5 using X-rays generated by a tube with Ti-target. The device is free of dark and bright pixels.

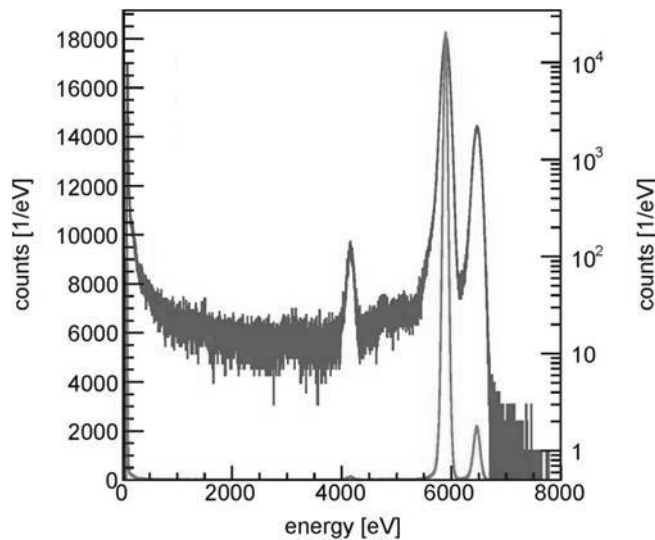


Figure 7. ⁵⁵Fe source spectrum recorded with the device shown in fig. 5 including all single events, in logarithmic and linear scale. The energy resolution at 5.9 keV is 132 eV FWHM. The device has been operated with only moderate cooling at -5 °C and with a signal processing time of 6 μs per row.

On the way towards the IXO Wide Field Imager, recently the pixel count has been increased significantly by the first measurement of a 256 x 256 pixel device developed in the context of the XEUS (X-ray Evolving Universe Spectroscopy) mission, one of the previous mission concepts now merged into IXO. XEUS had different mirror specifications with a smaller point spread function. Consequently, the pixel size of this device is 75 x 75 μm² and the sensitive area is 1.92 x 1.92 cm². Figure 5 shows a photograph of the sensor mounted on a hybrid substrate and wire-bonded to four ASTEROID readout chips and 8 SWITCHER control chips. The device has been operated with only moderate cooling at -5 °C and with a signal processing time of 6 μsec per row. The APS has no dead or noisy pixel and the uniformity of the

DePFET parameters is high: the gain and noise dispersions (1σ) are on the 2 % and 9 % level respectively. The sensor has been illuminated flat field and partially shadowed by a Silicon baffle (fig. 6) using a radioactive ^{55}Fe source (Mn-K lines at 5.9 and 6.5 keV) and an X-ray tube with a Titanium target (Ti-K line at 4.5 keV). ^{55}Fe spectra have been obtained by backside illumination. The width of the 5.9 keV line is 132 eV for single pixel hits (fig. 7) and 153 eV for all events including recovered two-, three, and four-fold split events. Further measurements accompanied by optimization of the readout speed and evolution of the data analysis are scheduled.

The next steps towards the IXO Wide Field Imager will be the adaptation of the pixel size to $100 \times 100 \mu\text{m}^2$ and a further increase of the sensor format to a WFU quadrant with 512×512 pixels and a sensitive area of more than 25 cm^2 . These devices are in production and will be available for tests at the beginning of 2011.

SUMMARY AND OUTLOOK

The planned Wide-Field Imager (WFI) of the International X-ray Observatory (IXO) is based on a Active Pixel Sensor (APS) built using DePFET pixel elements. Its monolithic implementation on a 6 inch wafer gives the WFI the maximum unobstructed field of view available. The DePFET technology employed enables the WFI to provide very high energy resolution while reading out at very high frame-rates. As the integrated signal of one pixel is not influenced by another pixel's read-out, even higher frame-rates are possible for reduced area regions of interest with very flexible read-out modes. The high data-rate generated by the APS requires fast, low-noise Analog Front End electronics and sophisticated on-board data reduction, both currently under development. Tests using existing DePFET matrices in a representative format and analog frontend prototypes have shown very promising results. Tests of larger physical and logical area prototypes and the production of very large WFI quadrant prototypes are under way.

REFERENCES

- [1] <http://ixo.gsfc.nasa.gov>
- [2] Kemmer J., Lutz G., "New semiconductor detector concepts", *Nucl. Instr. and Meth. A* **253** 365-377 (1987)
- [3] Treis J., Fischer P., Haelker O., Harter M., Herrmann S., Kohrs R., Krüger H., Lechner P., Lutz G., Peric I., Porro M., Richter R.H., Strüder L., Trimpl M., Wermes N., "DEPMOSFET Active Pixel Sensor Prototypes for the XEUS Wide Field Imager", *IEEE Trans. Nucl. Sci.* **52(4)** 1083-1091 (2005)
- [4] Bombelli L., Fiorini C., Ricca A.A., Porro M., Herrmann S., Wassatsch A., Treis J., "Fast DEPFET read-out for the Simbol-X low energy detector", *IEEE NSS Conference Record* **N21-3** 1772-1777 (2008)
- [5] De Vita G., Herrmann S., Porro M., Wassatsch A., Lauf T., Stefanescu A., Treis J., Bombelli L., Fiorini C., "64-channel ASTEROID ASIC: Experimental performance and measurements with Macro Pixel arrays for X-ray astronomy", *IEEE NSS Conference Record* **N23-6** 1096-1099 (2009)
- [6] Lechner P., Andricek L., Briel U., Hasinger G., Heinzinger K., Herrmann S., Huber H., Kendziorra E., Lauf T., Lutz G., Richter R., Santangelo A., Schaller G., Schneck M., Schopper F., Segneri G., Strüder L., Treis J., "The low energy detector of Simbol-X", *Proc. SPIE* **7021** 10.1-10.11 (2008)